# Interfacial Trap Density-of-States in Pentacene- and ZnO-Based Thin-Film Transistors Measured via Novel Photo-excited Charge-Collection Spectroscopy

By *Kimoon Lee, Min Suk Oh, Sung-jin Mun, Kwang H. Lee, Tae Woo Ha, Jae Hoon Kim, Sang-Hee Ko Park, Chi-Sun Hwang, Byoung H. Lee, Myung M. Sung,* and *Seongil Im**

Organic and oxide-based thin-film transistors (TFTs) have recently been expected to promote advances in display electronics based on low cost, high transparency, and flexibility.[1,2] The operational stabilities of such TFTs are thus important, strongly depending on the nature and density of charge traps present at the channel/dielectric interface or in the thin-film channel itself.[3–5] In particular, the illuminated display back panel is susceptible to the charge-trap-induced instability. Therefore the characterization of these traps is critical. Despite such immediate demands, appropriate methodologies to directly analyze the interfacial properties are quite rare, to the best of our knowledge, and conventional analysis techniques are rather unsatisfactory.[5] Photoluminescence (PL) is a direct method to observe deep-level defects in semiconductors but can not be used on a working device with interfaces.[6,7] Deep-level transient spectroscopy (DLTS) and gate-bias stress techniques may be used with working TFT devices to characterize the interface trap states, utilizing thermal and electrical energies, respectively.[7–11] However, DLTS is not adequate for organic based devices due to their thermal instability and gate-bias stress technique can never properly examine the electronic states of the deep-level traps. For instance Lang et al.[10] and Goldmann et al.[11] extracted the density-of-gap states from organic field-effect transistors (OFETs), obtaining the activation energy for trap charge release as a function of the gate bias. They quantitatively determined the total value of interfacial trap density, but only obtain the information on shallow level traps placed a few hundred meV above the valence band maximum (VBM). We here introduce a novel measurement technique, photo-excited trap-charge-collection spectroscopy, as a direct probe of the traps which utilizes the photo-induced threshold voltage ($V_{th}$) response of a working TFT device. Interface charges trapped at a certain energy level are liberated by the energetic photons and then electrically collected at the source/drain (S/D) electrodes. During this photo-electric process the $V_{th}$ or the onset voltage of TFTs is shifted. The magnitude of threshold voltage shift ($\Delta V_{th}$) provides us with a direct measure of the density-of-charge traps while the energy levels of those traps are simply scanned over by the photon energy. As a consequence, we can sensitively probe the fine density-of-states (DOS) profiles for detailed mid-gap states in the channel/dielectric interface of a working TFT device whether it has inorganic or organic channel.

**Figure 1a** illustrates the system schematics of photo-excited charge-collection spectroscopy to measure the photo-induced charge density generated in our top-gate transparent ZnO-TFT and bottom-gate pentacene-TFT. The system consist of a light source of 500 W Hg(Xe) arc lamp, a grating monochromator covering the spectral range of 254 ~ 1000 nm, an optical fiber (core diameter of 200 μm) as an optical probe which guides photons onto the channel of our TFT device, and a semiconductor parameter analyzer (Model HP 4155C, Agilent Technologies). Under an intense monochromatic photon beam (photon flux of at least $5 \times 10^{15}$ $cm^{-2}$ $sec^{-1}$ as estimated from the optical power density, 2 $mW \cdot cm^{-2}$), the transistor transfer curves were obtained from the TFTs engaged with electrical probes. Figure 1b displays the actual features of photo-excited charge-collection spectroscopy working for a top-gate transparent ZnO-TFT. We put our transparent TFT array with glass substrate on a black-color paper, to reveal the TFTs. As shown in Figure 1b, we used three electrical probes of source, drain, and gate, and one optical probe delivering energetic photons. For the photo-electric measurement, we applied sequentially mono-energetic photons onto our TFT device from low to high energy, to release the trapped charges at the channel/dielectric interface in the order from shallow to deep-level.

The photo-induced transfer characteristics for ZnO- and pentacene-TFTs are shown in **Figure 2a** and b, respectively, along with their dark transfer curves. A very low $V_D$ of 1 V was applied to the devices, so that the photo-charge collection proceeds in a very linear regime, not in saturation (to protect any probable measurement error by a large drain electric field). Gate bias

[*] K. Lee, S.-J. Mun, K. H. Lee, T. W. Ha, Prof. J. H. Kim, Prof. S. Im
Institute of Physics and Applied Physics
Yonsei University
262 Seongsanno, Seodaemun-gu, Seoul 120-749 (Korea)
E-mail: semicon@yonsei.ac.kr
Dr. M. S. Oh
Flexible Display Research Center
Korea Eletronics Technology Institute
68 Yatap-dong, Bundang-gu, Seongnam-si, Gyeonggi-do
463-816 (Korea)
Dr. S.-H. K. Park, Dr. C.-S. Hwang
IT Convergence and Component Lab.
Electronics and Telecommunications Research Institute
138 Gajeongro, Yuseong-gu, Daejeon 305-700 (Korea)
B. H. Lee, Prof. M. M. Sung
Department of Chemistry
Hanyang University
17 Haengdang-dong, Seongdong-gu, Seoul 133-791 (Korea)

DOI: 10.1002/adma.201000722

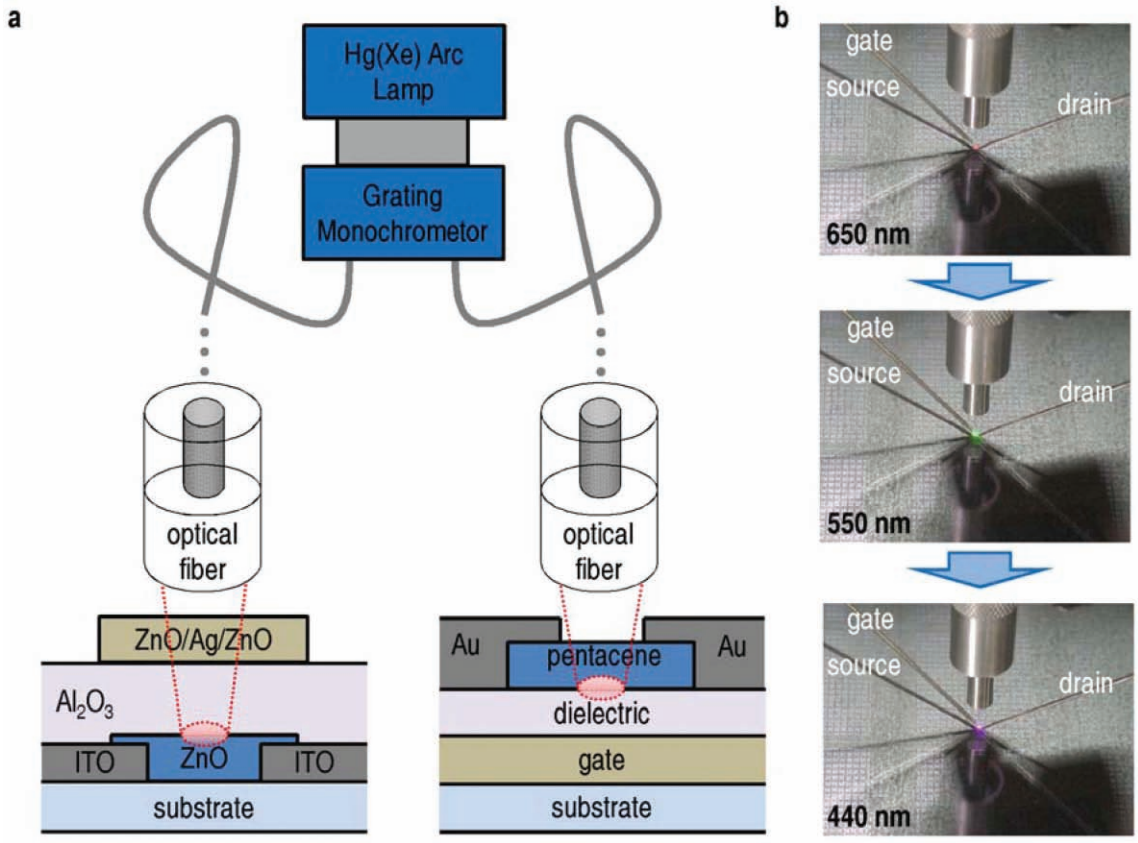


**Figure 1.** a) Measurement set-up: two kinds of working TFT devices (top-gate ZnO- and bottom-gate pentacene-TFT) and monochromatic illuminations to be delivered onto channel/dielectric interface by optical fiber probe. b) Photographic views of photo-excited charge-collection spectroscopy using monochromatic beams, among which red (650 nm), green (550 nm), and blue (440 nm) lights are operating on fully transparent ZnO-TFTs. We put our transparent TFT array on a black-color paper to reveal the TFTs.

sweep started from the channel accumulation state because we should initially fill up all the interface trap states with charge carriers prior to the photo-excitation process. If the TFT has an n-channel, the trap states are to be initially filled with electrons (Figure 2c), but if it is a p-channel TFT, the traps would be filled with holes and/or most of the electrons in the traps will be evacuated (Figure 2d). When the photo-excitation initiates, the trapped charge carriers are released into the band edges as indicated by the arrows. As shown in Figure 2a,b, $\Delta V_{th}$ as a function of photon energy was clearly observed in both the ZnO- and pentacene-TFTs while no significant changes in the sub-threshold slope ($S$), field-effect mobility ($\mu_{FET}$), and off-state drain current ($I_{off}$) values were observed. These photo-induced $\Delta V_{th}$ can be explained by electron transitions from electron-trap charge states (e.g. deep acceptor or deep donor in accumulation state) to the conduction band minimum (CBM) in the case of ZnO-TFT (Figure 2c) and by hole transitions from its hole-trap charge states to the valence band maximum (VBM) in the other case of pentacene-TFT (Figure 2d). When photons with a specific energy, $\varepsilon$, illuminate through the thin channel to reach the channel/dielectric interface of a TFT, most of the trap charges (electrons) in the gap states between CBM – $\varepsilon$ and CBM are excited to CBM level in the n-channel ZnO-TFT, since the number of incident photons (order of ~$10^{15}$ $cm^{-2}$) is large compared to that of trap states, which is far smaller (order of $10^{12}$ ~ $10^{13}$ $cm^{-2}$). Likewise most of the trapped holes in the gap states between VBM and VBM+$\varepsilon$ are excited to VBM level in the p-channel pentacene-TFT. This means that the effective trap charge ($Q_{eff}$), which is mainly for the traps remaining at the channel/dielectric interface, can be varied with photon energy $\varepsilon$, and then the photo-shifted $V_{th}$ can be represented by[3]

$$V_{th}(\varepsilon) = \phi_{ms} - \frac{Q_{eff}(\varepsilon)}{C_{ox}} + \psi_{s,max} + \frac{Q_G}{C_{ox}} \quad (1)$$

with

$$\begin{aligned} Q_{eff}(\varepsilon) &= q\int_{VBM}^{CBM-\varepsilon} D_{it,e}(E)F(E)dE - qN_bt_{ox} \\ &= q\int_{VBM}^{CBM-\varepsilon} D_{it,e}(E)dE - qN_bt_{ox} \quad for\ n-channel \\ &\quad q\int_{CBM}^{VBM+\varepsilon} D_{it,h}(E)\{1-F(E)\}dE - qN_bt_{ox} \\ &= q\int_{CBM}^{VBM+\varepsilon} D_{it,h}(E)dE - qN_bt_{ox} \quad for\ p-channel \end{aligned} \quad (2)$$

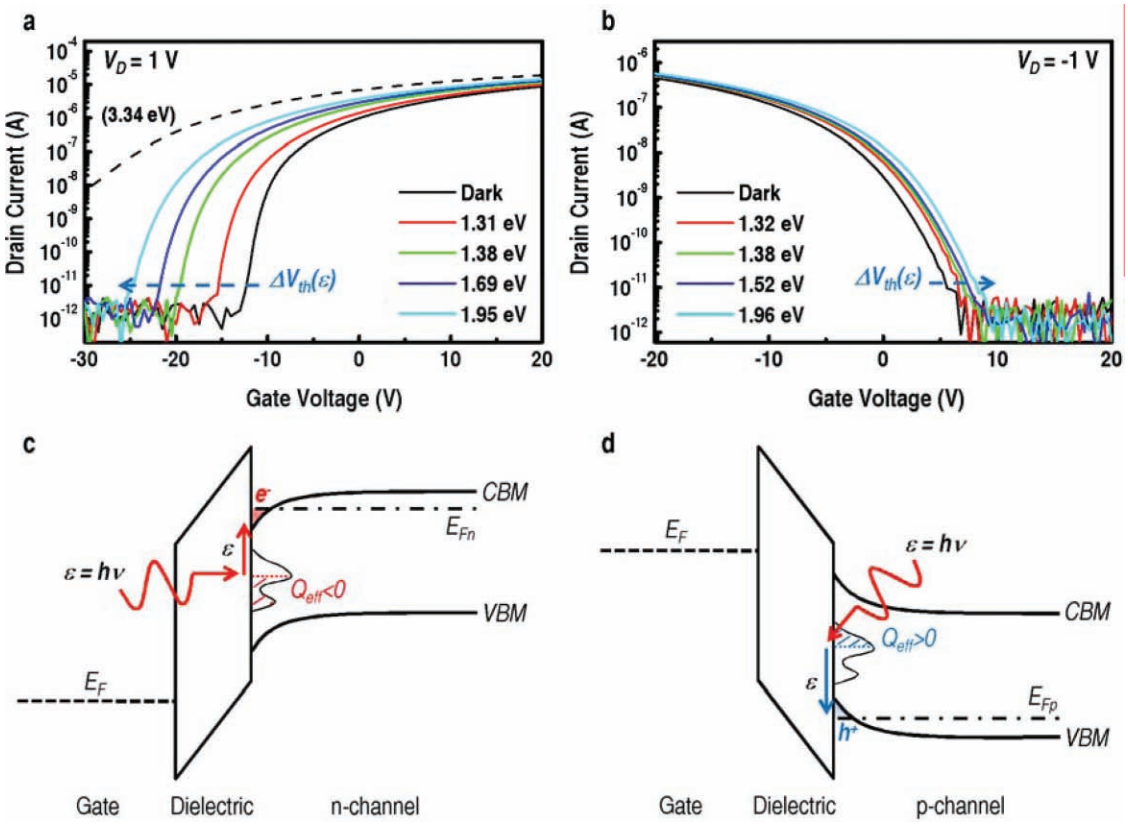


**Figure 2.** Static photo-induced transfer curves obtained from a) transparent ZnO-TFT and b) pentacene-TFT under several energetic photon beams. Energy band diagrams which elucidate the photo-excitation of c) electron-trap charges in n-channel ZnO-TFT and that of d) hole-trap charges in p-channel pentacene-TFT. Those excited charge carriers contribute to the abrupt shift of $V_{th}$ in the TFT devices. Red and blue shades represent remaining electron and hole charges trapped at the respective interfaces.

where $\phi_{ms}$ is the metal-semiconductor work function difference, $C_{ox}$ is the dielectric capacitance per unit area (F·cm$^{-2}$), $\psi_{s,max}$ is the potential due to band bending of the channel semiconductor, $Q_G$ is the charge associated with dielectric band bending as induced by gate bias, $N_b$ is the density (cm$^{-3}$) of bulk traps in the gate dielectric, $t_{ox}$ is the dielectric thickness (nm), $D_{it,e}$ is the DOS of electron traps at the n-channel/dielectric interface, $D_{it,h}$ is the DOS of hole traps at the p-channel/dielectric interface (cm$^{-2}$eV$^{-1}$), and $F(E)$ is the Fermi-Dirac distribution function whose value must be 1 for n-channel and 0 for p-channel (see the Fermi levels of n-channel ($E_{fn}$) and p-channel ($E_{fp}$) in Figure 2c and d. (We assumed 0 Kelvin step function for considering $F(E)$ in Equation 2). Since $\phi_{ms}$, $\psi_{s,max}$, and $Q_G$ in Equation 1 are rarely changed by $\varepsilon$, and since $N_b$ in Equation 2 also hardly varies with $\varepsilon$, photo-induced $\Delta V_{th}$ can be analyzed by taking a derivative of Equation 1 with $\varepsilon$, as shown below,

$$\frac{\partial V_{th}(\varepsilon)}{\partial \varepsilon} = -\frac{1}{C_{ox}} \frac{\partial Q_{eff}(\varepsilon)}{\partial \varepsilon} \tag{3}$$

and then by substituting Equation 2 into Equation 3, which now results in

$$\frac{\partial V_{th}(\varepsilon)}{\partial \varepsilon} = \frac{q}{C_{ox}} \left\{ D_{it,e}(CBM - \varepsilon) \right\} \quad for\ n-channel$$
$$-\frac{q}{C_{ox}} \left\{ D_{it,h}(VBM + \varepsilon) \right\} \quad for\ p-channel \tag{4}$$

If the bulk-trap densities in the both channel and dielectric oxide are negligible, $D_{it,e}$ $(CBM\text{-}\varepsilon)$ and $D_{it,h}$ $(VBM\text{+}\varepsilon)$ are determined, to be

$$D_{it,e}(CBM - \varepsilon) = \frac{C_{ox}}{q} \frac{\partial V_{th}(\varepsilon)}{\partial \varepsilon} \quad for\ n-channel$$
$$D_{it,h}(VBM + \varepsilon) = -\frac{C_{ox}}{q} \frac{\partial V_{th}(\varepsilon)}{\partial \varepsilon} \quad for\ p-channel \tag{5}$$

where $D_{it,e}$ $(CBM\text{-}\varepsilon)$ and $D_{it,h}$ $(VBM\text{+}\varepsilon)$ are the DOS (cm$^{-2}$eV$^{-1}$) with respect to CBM and VBM for n-channel and p-channel, respectively. Above equations from (3) to (5) show how we can eventually extract the information of $\Delta Q_{eff}$ $(\varepsilon)$ and DOS, which is not much difficult because $\Delta V_{th}$ $(\varepsilon)$ with respect to $\varepsilon$ is easily achievable from photo-induced transfer curves (experimental section shows more details). According to the Equation 5 it is worthwhile to note that if $\partial V_{th}/\partial \varepsilon < 0$ for n-channel (negative $V_{th}$ shift) and $\partial V_{th}/\partial \varepsilon > 0$ for p-channel (positive $V_{th}$ shift) with electronic charge ($q < 0$), the DOS values are always positive regardless of the channel type.

It should be again considered that this $D_{it}$ measurement by photo-induced $\Delta V_{th}$ with $\Delta\varepsilon$ is only valid in the case without much bulk trap density but with interface trap densities. If our oxide and organic devices with respective 20 nm- and 50 nm-thick channels show quite a density of bulk traps, their $S$, $\mu_{FET}$, and $I_{off}$ values should also change[13,14] because an

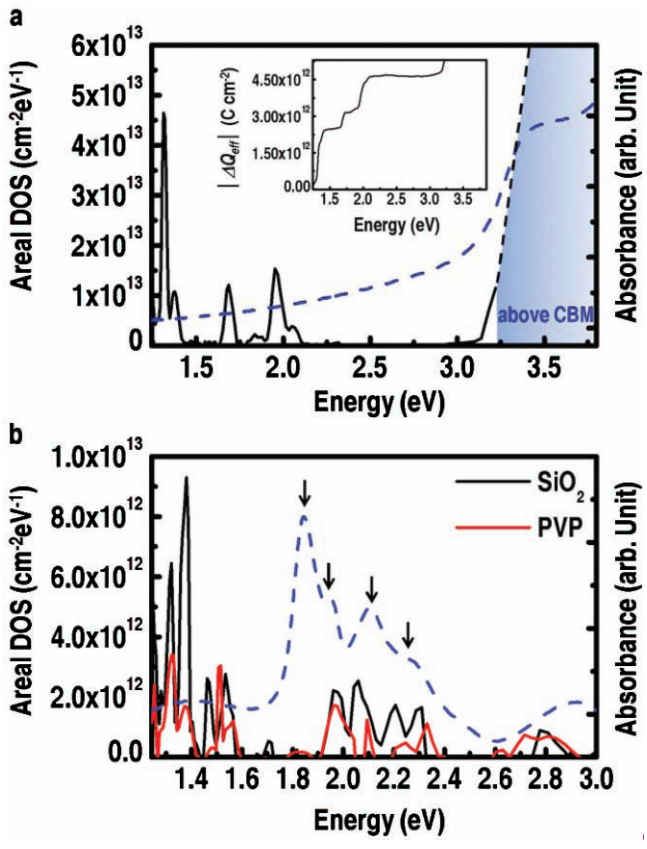


**Figure 3.** a) The DOS plot extracted from $|\Delta Q_{eff}(\varepsilon)|$ vs. $\varepsilon$ plot (inset) of ZnO-TFT. The plot was overlapped with an optical absorbance spectrum of $ZnO/Al_2O_3$ on glass (dashed blue), which was prepared for comparison. The DOS profile above CBM is too high to be measured. (The shaded region means "above CBM".) b) The obtained DOS plots for pentacene-TFTs with $SiO_2$ (solid black) and PVP (solid red) gate dielectric layer. The optical absorbance spectrum for pentacene/PVP on glass was measured (dashed blue), to be compared with the DOS profiles.

effective channel layer thickness is at most 5 nm from the interface. However, little change of those experimental factors was observed and now it confirms that our interfacial DOS evaluation is valid.[3,12,15] If a certain TFT has its $I_{off}$ level somewhat increase under photons, the DOS for its interface traps would not be easily distinguished from that of bulk traps.

**Figure 3a** and b show DOS profiles which were acquired by our photo-excited charge-collection spectroscopy for ZnO- and pentacene-TFTs, respectively. In Figure 3a we can observe a number of DOS ($cm^{-2}$ $eV^{-1}$) peaks which represent individual trap energy states in our ZnO-TFT while we also see the value of $|\Delta Q_{eff}(\varepsilon)|$ [= $|Q_{eff}$ (0) − $Q_{eff}$ $(\varepsilon)|$] increase with the photon energy, $\varepsilon$ in the inset of Figure 3a. Among the DOS peaks, several located at ~1.69 eV (peak intensity: $1.2 \times 10^{13}$ $cm^{-2}eV^{-1}$), ~1.84 eV ($2.3 \times 10^{12}$ $cm^{-2}eV^{-1}$), ~1.95 eV ($1.5 \times 10^{13}$ $cm^{-2}eV^{-1}$), and ~2.05 eV ($3.9 \times 10^{12}$ $cm^{-2}eV^{-1}$) matched incredibly well with the theoretical deep electron trap energy levels calculated by Janotti et al.,[16] respectively corresponding to $O_{Zn}$ (-/2-) (1.66 eV), $O_i$(oct) (-/2-) (1.84 eV), $O_{Zn}$ (0/-) (1.91 eV), and $Zn_O$ (4+/2+) (1.98 eV), which are located below the CBM of ZnO. (Here $O_{Zn}$: oxygen antisite, $O_i$(oct): oxygen interstitial occupying the octahedral interstitial site, $Zn_O$: zinc antisite). Those oxygen-rich trap levels possibly formed inside the ZnO film but near the $ZnO/Al_2O_3$ interface since oxygen plasma and water vapor were used as a precursor for ZnO and $Al_2O_3$ deposition during the atomic layer deposition (ALD) process. The most interesting peaks are found at ~1.31 and 1.38 eV below CBM with a large DOS peak intensity of $4.6 \times 10^{13}$ and $1.1 \times 10^{13}$ $cm^{-2}$ $eV^{-1}$, respectively. These peaks are apparently too deep to be considered as an oxygen vacancy ($V_O$) or a zinc interstitial state ($Zn_i$) in ZnO because the reported values are quite shallow to be 0.1 ($Zn_i$) and less than at most ~1 eV ($V_O$).[16] We thus regard those two peaks as the DOS of unknown interfacial traps which might be generated at $ZnO/Al_2O_3$ interface, but there must be further computational studies. When the photon energy approaches to the band gap of ZnO (~3.34 eV), the $\Delta V_{th}$ shoots up as shown with the dashed black curves of Figure 2a and 3a. The dashed blue curve is an optical absorbance spectrum of $ZnO/Al_2O_3$ (on glass) which was fabricated under the same experimental conditions, to be compared with the DOS profile. Large absorption was observed at similar photon energy levels near the CBM of ZnO. However, unlike the DOS profile, which was very sensitive to the interface traps, optical absorption could not resolve those trap levels located at the $ZnO/Al_2O_3$ interface.

The DOS plots for two types of pentacene-TFTs with $SiO_2$ (solid black) and with poly-4-vinylphenol (PVP) gate dielectrics (solid red) are shown in Figure 3b. Our photo-excited charge-collection spectroscopy again works equally well for organic pentacene-TFTs with pentacene/dielectric interface. Regardless of the type of dielectrics, the CBM state which is equivalent to the lowest unoccupied molecular orbital (LUMO) in organic semiconductors, was found at the same energy level, identified by a peak at ~1.96 eV, with similar DOS value of ~$2 \times 10^{12}$ $cm^{-2}eV^{-1}$ for both pentacene-TFTs. (Here the energy level is with respect to VBM or the highest occupied molecular orbital (HOMO)). The peak value is in good agreement with the HOMO-LUMO gap of solid pentacene.[17,18] Besides the HOMO-LUMO level, a few other molecular levels above the HOMO-LUMO were always observed at ~2.1, ~2.2, and ~2.3 eV in our DOS profiles. These features are the replica found from the (arrow-indicated) exciton peaks of optical absorbance spectra of a solid pentacene film (blue dashed line), but some energy deviation between optical gap and HOMO-LUMO gap is shown due to the high exciton binding energy over 0.1 eV in pentacene.[17] However, the most important spectroscopic results from our photo-excitation method may be the DOS peaks observed at ~1.32 and ~1.38 eV. The DOS peaks are clearly observed for both pentacene-TFTs with PVP and $SiO_2$ dielectrics although the peaks are much smaller in the case of the device with PVP. Those two energy levels have not been reported but must be the states of deep hole traps although they are found above HOMO but quite near LUMO level. Those levels can not be resolved with optical absorption, which is not interface-sensitive. This again means that our photo-excited charge-collection spectroscopy is highly sensitive to interfacial traps.

Since the measured DOS profiles of pentacene-TFTs in Figure 3b provide a very important insight that the hydrophobic PVP dielectric produces a much lower density of deep hole traps at the interface than in the case of hydrophilic $SiO_2$, we fabricated a completely photo-stable organic TFT with a highly

hydrophobic dielectric as a practical application of our photo-excited charge-collection spectroscopy. The ALD-growth of our 60 nm-thin $Al_2O_3$ dielectric was performed on a patterned indium-tin-oxide (ITO) gate, to realize low voltage operating pentacene-TFTs. Then, the surface of $Al_2O_3$ was functionalized, in the order of hydrophobicity, with self-assembled-monolayers (SAMs) of Hexamethyldisilazane (HMDS), 7-octenyltrichlorosilane (7-OTS), and Trichloro(1H,1H,2H,2H-perfluorooctyl) Silane (FTS). Figure S1 displays the lowering of trap densities or trap DOS peaks in the order of hydrophobicity of the dielectric surface. As a matter of fact, this photo-electric stability of channel/dielectric interface is deeply related to the dark electrical stability as well. For example, under long-term negative gate bias stress or repeated gate bias sweep in the dark, more holes are possibly trapped at the pentacene/dielectric interface, so that most of the devices with trap-containing petacene/$Al_2O_3$ interface might exhibit rather unstable time-dependent behavior while our FTS-treated device displayed very stable features (see Figures. S2(a) and (b)). Please note the arrow in Figure S2(a) which indicates $V_{th}$ shift by the bias-induced trapping. (The arrow direction is opposite to the case of photo-induced trap releasing (Figure 2b). These results coincide with the recent reports that some hydrophobic dielectric surface induces the electrical stability for OFETs.[19,20]

In summary, we have invented photo-excited charge-collection spectroscopy as a new methodology to quantitatively measure the DOS of interfacial deep traps in working TFTs, applying the spectroscopy to both inorganic and organic channel TFTs. The photo-induced $\Delta V_{th}$ successfully quantified the profile of the DOS of deep-level defects located at or near the channel/dielectric interface. Inspired by the spectroscopy results, we have also fabricated a very photo-stable trap-minimized pentacene-TFT which operates at low voltage. We anticipate that our photo-excited charge-collection spectroscopy will be a reliable probe to measure the interface quality and photo-stability of a working TFT but also will be a powerful characterization tool to understand the nature of interfacial traps.

## *Experimental Section*

*Fabrication of ZnO-Based Transparent TFTs*: For the fabrication of transparent ZnO-TFT array, a 150 nm-thick ITO glass was used for the substrate. After S/D patterning of ITO by wet etching, 20 nm-thin ZnO semiconductor film was deposited by means of plasma-enhanced atomic layer deposition (PEALD), which uses diethylzinc (DEZ) and oxygen plasma (RF power ~130 W) as the Zn and oxygen precursors, respectively, at the substrate temperature of 200 °C. A 160 nm-thick top $Al_2O_3$ gate dielectric and transparent electrode processes were previously introduced elsewhere in detail.[2] Width-to-length (W/L) of our device was 40 μm/20 μm. Our fabricated fully transparent ZnO-TFTs showed a good mobility of ~4 $cm^2$/V s and an excellently high on/off ratio of ~$10^7$ with high transparency of ~80 % in visible range.

*Fabrication of Pentacene-Based TFTs*: The both substrates of ITO/glass and heavily-doped silicon ($p^+$-Si) were cleaned with acetone, methanol, and de-ionized water, in that order. In the case of PVP and $Al_2O_3$ dielectrics, ITO gate electrodes were patterned by wet etching. 230 nm-thick PVP films were prepared from solutions of PVP and polymelamine-co-formaldehyde, as a cross-linking agent, in propylene glycol monomethyl ether acetate, by spin coating and subsequent cross-linking (curing) at 175 °C for 1 h in a vacuum oven.[21] For inorganic dielectric, we used 200-nm-thick conventional thermally grown $SiO_2$ on $p^+$-Si and ALD-grown 60 nm-thin $Al_2O_3$ on patterned ITO glass. The surfaces of $Al_2O_3$ were functionalized with SAMs of HMDS, 7-OTS, and FTS.[22] Pentacene (Aldrich Chem. Co., 99% purity, no other distillation) active channel layers were patterned on the dielectric layers through a shadow mask by thermal evaporation at room temperature (RT). The final pentacene thickness was 50 nm. For S/D of the pentacene-TFTs, Au was then evaporated onto the pentacene channels at RT. Nominal channel length ($L$) and width ($W$) of our pentacene-TFTs were 90 and 500 μm, respectively.

*Photo-Excited Charge-Collection Spectroscopy*: The system consists of a light source of 500 W Hg(Xe) arc lamp, a grating monochromator covering the spectral range of 254 ~ 1000 nm, an optical fiber (core diameter of 200 μm), and a semiconductor parameter analyzer (Model HP 4155C, Agilent Technologies). From the dark and photo-induced transistor transfer curves we measured $\Delta V_{th}$. The wavelength of selected photons started from 1000 nm (the lowest energy) for the photo-induced transfer curves and was decreased by 5 nm for the next transfer curve. The wavelength was converted to eV for the $|\Delta Q_{eff}(\varepsilon)|$ [= $|Q_{eff}(0) - Q_{eff}(\varepsilon)|$] (= $|C_{ox}\Delta V_{th}|$) vs. $\varepsilon$ (eV) or DOS vs. $\varepsilon$ (eV) plots.

## Supporting Information

Supporting Information is available online from Wiley InterScience or from the author.

## Acknowledgements

The authors acknowledge the financial support from NRF (Program No. 2009-8-0403), the IT R&D Program of MKE (Program No. 2008-8-0613, Smart window with transparent electronic devices) and Brain Korea 21 Program. K. Lee acknowledges the support from the National Graduate Science and Technology Scholarship, Republic of Korea.

Received: February 27, 2010
Published online: June 1, 2010

[1] S. R. Forrest, *Nature* **2004**, *428*, 911.
[2] S. H. K. Park, C. S. Hwang, M. Ryu, S. Yang, C. Byun, J. Shin, J. I. Lee, K. Lee, M. S. Oh, S. Im, *Adv. Mater.* **2009**, *21*, 678.
[3] a) J. Jang, in *Thin-Film Transistors* (Eds: C. R. Kagan, P. Andry), Marcel & Dekker, Inc, New York **2003**, Ch. 2; b) A. T. Voutsas, M. K. Hatalis in *Thin-film Transistors*, (Eds: C. R. Kagan, P. Andry), Marcel & Dekker, Inc, New York **2003**, Ch. 4.
[4] H. Sirringhaus, *Adv. Mater.* **2009**, *21*, 3859.
[5] D. Gracias, *Nat. Photon.* **2007**, *1*, 570.
[6] T. M. Borseth, B. G. Svensson, A. Y. Kuznetsov, P. Klason, Q. X. Zhao, M. Willander, *Appl. Phys. Lett.* **2006**, *89*, 262112.
[7] R. S. Wang, Q. L. Gu, C. C. Ling, H. C. Ong, *Appl. Phys. Lett.* **2008**, *92*, 042105.
[8] H. Frenzel, H. v. Wenckstern, A. Weber, H. Schmidt, G. Biehne, H. Hochmuth, M. Lorenz, M. Grundmann, *Phys. Rev. B* **2007**, *76*, 035214.
[9] Y. S. Yang, S. H. Kim, J. I. Lee, H. Y. Chu, L. M. Do, H. Lee, J. Oh, T. Zyung, M. K. Ryu, M. S. Jang, *Appl. Phys. Lett.* **2002**, *80*, 1595.
[10] D. V. Lang, X. Chi, T. Siegrist, A. M. Sergent, A. P. Ramirez, *Phys. Rev. Lett.* **2004**, *93*, 086802.
[11] C. Goldmann, C. Krellner, K. P. Pernstich, S. Haas, D. J. Gundlach, B. Batlogg, *J. Appl. Phys.* **2006**, *99*, 034507.
[12] S. M. Cho, S. H. Han, J. H. Kim, J. Jang, M. H. Oh, *Appl. Phys. Lett.* **2006**, *88*, 071106.
[13] T.-C. Fung, C.-S. Chuang, K. Nomura, H.-P. D. Shieh, H. Hosono, J. Kanicki, *J. Inf. Disp.* **2008**, *9*, 21.

[14] K. Wasapinyokul, W. I. Milne, D. P. Chua, *J. Appl. Phys.* **2009**, *105*, 024509.
[15] W. Eccleston, *IEEE Trans. Electron Devices* **2006**, *53*, 474.
[16] A. Janotti, C. G. V. de Walle, *Phys. Rev. Lett.* **2007**, *76*, 165202.
[17] J. Lee, S. S. Kim, K. Kim, J. H. Kim, S. Im, *Appl. Phys. Lett.* **2004**, *84*, 1701.
[18] T. Cramer, T. Steinbrecher, T. Koslowski, D. A. Case, F. Biscarini, F. Zerbetto, *Phys. Rev. B* **2009**, *79*, 155316.
[19] W. L. Kalb, T. Mathis, S. Hass, A. F. Stassen, B. Batlogg, *Appl. Phys. Lett.* **2007**, *90*, 092104.
[20] M. P. Walser, W. L. Kalb, T. Mathis, T. J. Brenner, B. Batlogg, *Appl. Phys. Lett.* **2009**, *94*, 053303.
[21] D. K. Hwang, K. Lee, J. H. Kim, S. Im, J. H. Park, E. Kim, *Appl. Phys. Lett.* **2006**, *89*, 093507
[22] J. M. Choi, S. H. Jeong, D. K. Hwang, S. Im, B. H. Lee, M. M. Sung, *Org. Electron.* **2009**, *10*, 199.